AGU PUBLICATIONS

Water Resources Research

RESEARCH ARTICLE
10.1002/2013WR014942

A parameter estimation framework for Multiscale Kalman Smoother algorithm in precipitation data fusion

Shugong Wang[1,2] and Xu Liang[3]

[1]Science Applications International Corporation, McLean, Virginia, USA, [2]Hydrological Sciences Laboratory, NASA Goddard Space Flight Center, Greenbelt, Maryland, USA, [3]Department of Civil and Environmental Engineering, University of Pittsburgh, Pittsburgh, Pennsylvania, USA

Key Points:
- A multiobjective parameter estimation scheme for multiscale precip data fusion
- Comparison to widely used maximum likelihood parameter estimation algorithm
- The proposed scheme produced much better precipitation data at fine resolutions

Correspondence to:
X. Liang,
xuliang@pitt.edu

Citation:
Wang, S., and X. Liang (2014), A parameter estimation framework for Multiscale Kalman Smoother algorithm in precipitation data fusion, *Water Resour. Res.*, *50*, 8675–8693, doi:10.1002/2013WR014942.

Received 1 NOV 2013
Accepted 18 SEP 2014
Accepted article online 23 SEP 2014
Published online 12 NOV 2014

Abstract A new effective parameter estimation approach is presented for the Multiscale Kalman Smoother (MKS) algorithm. As demonstrated, it shows promising potentials in deriving better data products involving sources from different spatial scales and precisions. The proposed approach employs a multiobjective parameter estimation framework, which includes three multiobjective estimation schemes (MO schemes), rather than using the conventional maximum likelihood scheme (ML scheme), to estimate the MKS parameters. Unlike the ML scheme, the MO schemes are not built on strict statistical assumptions related to prediction errors and observation errors, rather, they directly associate the fused data of multiple scales with multiple objective functions. In the MO schemes, objective functions are defined to facilitate consistency among the fused data at multiple scales and the input data at their original scales as well in terms of spatial patterns and magnitudes. Merits of the new approach are evaluated through a Monte Carlo experiment and a series of comparison analyses using synthetic precipitation data that contain noises which follow either the multiplicative error model or the additive error model. Our results show that the MKS fused precipitation performs better using the MO framework. Improvements are particularly significant for the fused precipitation associated with fine spatial resolutions. This is due mainly to the adoption of more criteria and constraints in the MO framework. The weakness of the original ML scheme, arising from its blindly putting more weights into the data associated with finer resolutions, is circumvented in the proposed new MO framework.

1. Introduction

Most of weather-driven environmental simulations require reliable precipitation data as input, which significantly affect terrestrial water and energy budget, land-atmosphere interactions, ecological processes and some biogeochemical processes. The quality of precipitation data has direct and essential impacts on the reliability and applicability of simulation results. However, none of the precipitation data are good enough to completely satisfy the expectations of environmental simulations, which is mainly due to the limits associated with precipitation measurements, typically including rain gauges, weather radars and weather satellites. Rain gauges are reliable at local points but poor at capturing spatial patterns of the precipitation. On the contrary, weather radars are good at capturing spatial patterns but not that good in terms of the magnitudes. Moreover, weather radars have limited spatial coverage and do not work well in mountainous regions. Weather satellites have extensive spatial coverage but present uneven spatial and temporal resolutions. For example, the polar orbit satellites with microwave imagers measure precipitation at higher spatial resolutions but lower temporal resolutions, while the geostationary orbit satellites with infrared imagers result in data with coarser spatial resolutions but finer temporal resolutions. In addition to the representability of measurement instruments, uncertainty is another issue of the precipitation data, even for those produced with cutting-edge technologies, such as satellite-borne sensors [*Tian and Peters-Lidard*, 2010]. To improve the environmental simulations, it is fundamentally important to derive precipitation data products with better representability and lower uncertainty through data fusion in which multiple precipitation measurements, and simulated precipitation by numerical weather models, are effectively combined.

Fusion of the precipitation data is generally associated with multiple scales due to two reasons: (1) sensors available for precipitation measurements are associated with multiple spatial scales; and (2) data processing algorithms and weather/climate models are usually operated at different scales. Additionally, environmental

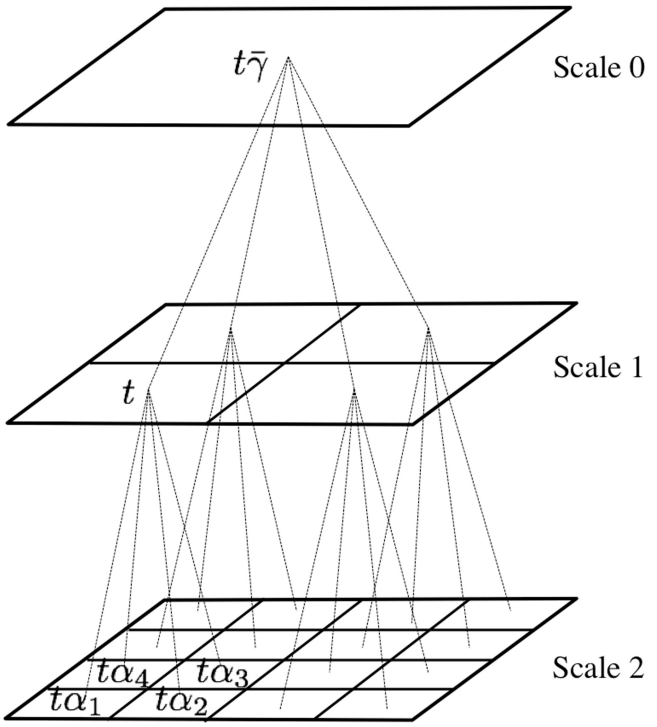

Figure 1. An example of multiscale tree: a two-dimensional multiscale tree with three spatial scales. For node t at scale 1, $t\bar{\gamma}$ represents its parent node and $t\alpha_n$ ($n=1, 2, 3, 4$) represents its child nodes. Without a parent, the node at scale 0 (i.e., the coarsest resolution) is called a root node; without any child nodes, the nodes at scale 2 (i.e., the finest resolution) are called leaf node.

applications may require precipitation data at yet another spatial scale. Thus, data fusion algorithms for precipitation should be able to deal with input and output data at multiple scales. Furthermore, fusion of the data from different sources with different scales should make it possible to extract useful information of different sources and then have the information effectively combined to form a new data set at the same or different spatial scales for applications. This would be especially beneficial for hydrological and land surface simulations. The current precipitation data products may be good at either spatial patterns or magnitudes but hardly at both [*Jayakrishnan et al*., 2004; *Voisin et al*., 2008]. For example, the precipitation data product of the National Weather Service (NWS) Next Generation Weather Radar (NEXRAD) Multisensor Precipitation Estimation (MPE) has a fine spatial resolution of 4 km, which is favorable in describing spatial patterns of the precipitation. However, it is noisy and sometimes has large biases in terms of its magnitude compared to the rain gauge measurements [*Wang et al*., 2008; *Nan et al*., 2010]. On the other hand, precipitation data products of North American Land Data Assimilation System (NLDAS) are better at describing magnitude since they are determined based on Climate Prediction Center (CPC) daily gauged precipitation data [*Cosgrove et al*., 2003]. But they are not very good at describing the spatial patterns due to their relatively coarse spatial resolution, e.g., 0.125°. It is reasonable to infer that more reliable precipitation data products can be derived by combining the NEXRAD MPE data with the NLDAS data through a multiscale data fusion approach [*Nan et al*., 2010]. Moreover, if precipitation data products at multiple spatial resolutions are required, the advantages of employing a multiscale precipitation fusion approach become obvious.

Among the data fusion algorithms such as artificial neural network [*Sorooshian et al*., 2000], Kalman Filter [*Smith and Krajewski*, 1991; *Ushio et al*., 2009] and statistical methods [*Ly et al*., 2011], the MKS algorithm [*Chou and Willsky*, 1991; *Chou et al*., 1994; *Willsky*, 2002; *Parada and Liang*, 2004] offers many good features which are particularly important for conducting the multiscale precipitation data fusion as illustrated in [*Wang et al*., 2011] through a systematic investigation and analyses. The MKS algorithm is based on the theory of Markov random field over space. It can easily fuse multiresolution (multiscale) data organized by a quadtree, as shown in Figure 1. With this MKS algorithm, fused precipitation at any scale represented by the quadtree can be derived. The MKS algorithm, also bearing the name of scale-recursive estimation (SRE) method, has been examined in multiscale precipitation data fusion applications and demonstrated great potentials. For example, *Gorenburg et al*. [2001] evaluated the SRE method in the assimilation of radar precipitation data and satellite precipitation data, which are at 2.5 km and 15 km respectively. The SRE method was able to reproduce withheld radar measurements through the fused precipitation data. Such kind of evaluation has also been done by *Van de Vyver and Roulin* [2009] with precipitation data of weather radar and satellite microwave measurements. Similarly, *Bocchiola* [2007] examined SRE method upon fusing precipitation measurements of TMI radiometer and PR radar boarded on the TRMM satellite and NEXRAD radar. In addition to studies in the spatial domain, SRE method has also been evaluated in the time domain to fuse precipitation data at varying temporal resolutions [*Tustison et al*., 2002]. Moreover, the MKS algorithm

has also been applied to soil moisture data assimilation [*Kumar*, 1999; *Parada and Liang*, 2004, 2008], altimetry data fusion [*Slatton et al*., 2001, 2002] and imagery data fusion [*Huang et al*., 2002; *Simone et al*. 2000]. A comprehensive review is provided by *Montzka et al*. [2012] for conducting data assimilation and data fusion for the terrestrial system in which the strength of the MKS-based algorithm [e.g., *Parada and Liang*, 2004; *Wang et al*., 2011] for multiscale data assimilation and fusion is discussed. In fact, all of the studies have shown that more reliable data products can be derived with the MKS-based algorithm by fusing or assimilating multiscale data if the algorithm parameters are determined properly.

MKS is an algorithm with high degree of freedom due to its relatively large number of parameters, which are involved in characterizing measurement errors, prediction errors and state-space equations. Performance of the MKS algorithm, like other algorithms, depends critically on proper estimations of these parameters. The Maximum Likelihood (ML) based methods are typically used to estimate parameters of the MKS algorithm because of its simple statistical formulation and high computational efficiency [*Chou*, 1996; *Digalakis et al*., 1993; *Bocchiola*, 2007]. Applying the Expectation-Maximization (EM) method, parameters of the MKS algorithm can be determined through iterations when there are latent variables involved in the MKS model framework [e.g., *Kannan et al*., 2000; *Parada and Liang*, 2004; *Gupta et al*., 2006]. However, it is quite often that both the ML and EM methods only find local optima but not global optima in practical applications. This is mainly because the ML and EM methods assume that the measurement errors and prediction errors are independent and follow zero-mean Gaussian distributions. Such assumptions make the derivation of the likelihood functions straightforward and simple to implement, but they are too strong to be generally satisfied by the precipitation data. This shortcoming hinders the MKS algorithm from fusing the precipitation data optimally at all spatial scales when the ML method is applied in combination with the EM method, as illustrated and discussed in [*Wang et al*., 2011]. In fact, *Wang et al*. [2011] showed that the fused precipitation data were significantly improved at the coarse resolution (e.g., 1/8°) while the improvement at the fine resolution (e.g., 1/32°) is limited or even deteriorated if the finer resolution data are much noisier than the coarse resolution data. This is due to a combined effect that only local optimal parameters are found and that too much weight is placed on the finer resolution precipitation data by the EM method associated with the MKS algorithm, which is fine if the data's noisy levels at the different scales are comparable. In this study, we present a new framework to improve the parameter estimations for the MKS algorithm so that the weakness of the ML method is circumvented or at least mitigated while the strength of the ML method is kept and that the improvements are achieved at multiple scales (i.e., at both coarse and fine scales).

The new parameter estimation framework is primarily designed to improve the performance of the MKS algorithm at finer resolutions in the multiscale data fusion applications. The new framework is based on a multiobjective optimization approach, and comprises three schemes that are referred as MO framework or MO schemes. Similarly, we refer the EM method that is used to estimate the maximum likelihood parameters of the MKS algorithm as ML scheme. Different from maximizing only a log-likelihood function in the ML scheme, the MO framework maximizes a number of objective functions, which are metrics directly related to the objectives of the multiscale precipitation data fusion. To solve the multiobjective optimization problem investigated in this study, we use a multiobjective particle swarm optimization (MOPSO) algorithm. The particle swarm optimization (PSO) algorithm was firstly proposed by *Kennedy and Eberhart* [1995]. MOPSO has been shown to be effective and efficient for optimizing hydrological parameters [*Gill et al*., 2006] for different multiobjective optimization problems [*Hu and Eberhart*, 2002; *Hu et al*., 2003]. In this study, we have designed and implemented a parallel MOPSO algorithm to solve the resulting multiobjective optimization problem.

In the remaining part of this paper, a brief description of the MKS algorithm and the EM scheme is provided in section 2 to have this paper self-contained. Detailed description and formulation of the MO framework are presented in section 3. Evaluations of the MO schemes are presented in section 4 through a Monte Carlo experiment and a series of comparison experiments that make use of both the multiplicative error and additive error models. Discussions and conclusions of this study are provided in section 5.

2. Descriptions of the MKS Algorithm and the ML Scheme

2.1. The MKS Algorithm

The MKS algorithm is able to fuse multidimensional data or one-dimensional data. In this study, the MKS algorithm is applied to the one-dimensional precipitation data, which means each value represents the

precipitation amount of one grid at one time instance. In the following mathematical descriptions, all notations represent scalars instead of vectors. In this study, a scale means a spatial resolution of the precipitation data. The MKS algorithm includes a fine-to-coarse sweep of the Kalman filtering step and a coarse-to-fine sweep of the Kalman smoothing step. Both sweeps are conducted along a multiscale tree, as shown in Figure 1. In the scale domain, a linear state-space model that relates measurements at neighboring resolutions is given as follows:

$$X(t)=A(t)X(t^{\bar{\gamma}})+w(t) \tag{1}$$

$$P(t)=A^2(t)P(t^{\bar{\gamma}})+Q(t) \tag{2}$$

where $X(t)$ and $X(t^{\bar{\gamma}})$ represent the precipitation estimates at a child node and its parent node, respectively, $w(t)$ is the prediction error following $\mathcal{N}(0,Q(t))$, $Q(t)$ is the variance of $w(t)$, $P(t)$ and $P(t^{\bar{\gamma}})$ are the error variances of $X(t)$ and $X(t^{\bar{\gamma}})$, and $A(t)$ is a transition operator mapping precipitation amount from a parent node to a child node.

Given the prior estimates of the precipitation amount at the root node $X(0)$ and the associated error variances, the unconditional estimates of precipitation and their error variances at the remaining nodes of the multiscale tree can be computed using equations (1) and (2). Such a step is referred as initialization. After that, an upward sweep is conducted from the leaf nodes toward the root node with the inverted forms of equations (1) and (2) and a measurement equation

$$Y(t)=C(t)X(t)+D(t)+v(t) \tag{3}$$

where $Y(t)$ is the measurement at node t, $C(t)$ is a transition operator mapping estimated precipitation amount to the measurement, $D(t)$ is a bias compensation term, and $v(t)$ is the variance of measurement error following $\mathcal{N}(0,R(t))$ where $R(t)$ is the error variance of $v(t)$. The $D(t)$ term is introduced to minimize impacts of the inconsistency (e.g., bias) among measurements at different scales on the fused precipitation [*Parada and Liang*, 2004; *Wang et al.*, 2011]. This step is the Kalman filtering at the spatial scale domain. Once it is done, all unconditional estimates of the precipitation have been updated according to measurements through which the finer resolution measurement data add their influences to the estimates of the precipitation at coarser resolutions. Following the upward sweep, a downward sweep is conducted from the root node toward the leaf nodes to refine the precipitation estimates by including the influences of the measurement data at coarser resolutions through Kalman smoothing. For a complete formulation of the MKS algorithm for general purposes, readers are referred to *Kannan et al.* [2000] and *Parada and Liang* [2004].

In a simple case that measurements are available at all nodes of a multiscale tree (denoted with $\mathcal{T}$), the MKS algorithm has a set of parameters, including $\Sigma(0)$ (initial value of the error variance of the root node $P(0)$) and $\{A(t),C(t),Q(t),R(t)|t\in\mathcal{T}\}$. Since all measurements have been converted into precipitation amounts, we can set $A(t)=1.0$ and $C(t)=1.0$ for all nodes in the precipitation data fusion application. However, the rest of the parameters, namely $\Sigma(0)$, $R(t)$ and $Q(t)$ need to be estimated. In reality, $R(t)$ and $Q(t)$ may vary over space. If $R(t)$ and $Q(t)$ are to be estimated at every node, the number of parameters would be more than the number of measurements, i.e., the number of nodes with valid measurements. In this instance, it would be hard to adequately estimate the parameters. In order to resolve this issue, we assume that $R(t)$ and $Q(t)$ are scale homogeneous. In other words, they are, respectively, identical for each node at the same scale. Consequently, the number of parameters is significantly reduced and is much lower than the number of measurements. The parameters can thus be estimated based on the available measurements without any further assumptions or constraints.

2.2. The ML Scheme

Assuming that the relationships described by equations (1) and (2) are independently held at all nodes of a multiscale tree ($\mathcal{T}$), the log-likelihood function can be expressed as follows, where we denote the parameter set of the MKS algorithm as θ ($\theta=\{X(0),\Sigma(0),R(t),Q(t)|t\in\mathcal{T}\}$)

$$\begin{aligned}\mathcal{L}(X,Y|\theta)=&-\frac{1}{2}\sum_{t\in\mathcal{T}_c}\{\log(Q(t))+[X(t)-A(t)X(t^{\bar{\gamma}})]^2Q(t)^{-1}\}\\&-\frac{1}{2}\sum_{t\in\mathcal{T}_m}\{\log(R(t))+[Y(t)-C(t)X(t)-D(t)]^2R(t)^{-1}\}+F\end{aligned} \tag{4}$$

where $\mathcal{T}_c$ represents a subset of $\mathcal{T}$ except the root node, $\mathcal{T}_m$ represents a subset of $\mathcal{T}$ with measurements, Y represents measurements, and F is a constant. Given measurements Y, precipitation estimates X are dependents of the parameter set θ. Therefore, $\mathcal{L}(X, Y|\theta)$ can be regarded as a function of θ with given measurements and accordingly θ can be estimated by maximizing $\mathcal{L}(X, Y|\theta)$.

In the ML scheme, parameter set θ is determined using the EM algorithm, which includes an expectation step (E-step) and a maximization step (M-step). In the multiscale precipitation data fusion applications, one cycle of the upward sweep and the downward sweep of the MKS algorithm serves as the E-step, which computes smoothed estimates of precipitation as statistical expectation. After the E-step, parameters θ are the only free variables in $\mathcal{L}(X, Y|\theta)$. The M-step is to maximize the log-likelihood (equation (4)) by adjusting the parameters using a numerical approach, such as gradient-based methods. Details about the ML scheme with the EM algorithm can be found in *Kannan et al*. [2000].

3. Multiobjective (MO) Parameter Estimation Framework

Our MO framework for the MKS algorithm is explicitly constructed on the expectation of multiscale precipitation data fusion. Generally, multiscale precipitation data fusion is to derive new precipitation products, which are expected to be better in representing the spatial patterns and magnitudes of the precipitation at the original scales of the input data or at any other scales depending on applications. But, on the other hand, these fused data sets should also be expected to inherit the characteristics of the spatial patterns and the magnitudes of their original data where appropriate. In principle, if the parameters of the MKS algorithm are reasonably estimated to represent the errors associated with each data source, then the spatial patterns and magnitudes of the fused precipitation data should be consistent with each other at all output scales. However, due to the limitations discussed in section 1, neither the popular maximum likelihood method nor the EM method is sufficiently effective in finding the MKS parameters in practical applications because the maxima obtained are local, and the methods usually overweigh observations from finer resolutions. Our idea is thus to force the search to find a better parameter set by introducing more physically sound constraints. To this end, we introduce two objective functions related to spatial patterns for a typical case of fusing two data sources. To avoid over smoothing, we also introduce some other objective functions to maximize maximum precipitation or maximum information in the fused precipitation data.

In a multiscale precipitation data fusion, the consistency in spatial patterns among output scales can be measured either with correlation (Corr) or root mean square error (RMSE). The former focuses more on spatial patterns while the latter focuses more on magnitudes. Correlation has intuitive statistical meaning and fixed lower and upper boundaries, i.e., -1.0 and 1.0. For a condition of having no biases, correlation usually has an approximately monotonic relationship with RMSE in the multiscale precipitation data fusion using our MKS algorithm [*Parada and Liang*, 2004] since the bias is mainly removed by the D term in equation (3) as demonstrated in *Wang et al*. [2011]. That is, for the same data, RMSE decreases with an increase in Corr. Therefore, correlation would be a proper measure of the consistency among fused precipitation data.

In order to calculate the correlation of two data sets associated with two different spatial scales (e.g., 1/8° and 1/32°), one can either aggregate the finer resolution data of 1/32° into the coarser resolution (i.e., 1/8°) or disaggregate the coarser resolution data of 1/8° into the finer resolution (i.e., 1/32°). Subsequently, one can calculate the correlations at both of these resolutions. In this study, we try to obtain the correlation as high as possible between two fused precipitation data sets at 1/8°. For example, a value of 1.0 indicates that the finer fused precipitation data (e.g., 1/32°) has a perfect consistency with the fused precipitation data at the coarser resolution (e.g., 1/8°). For the correlation at 1/32°, we try to have the correlation between the two fused precipitation data fields close to a target correlation value, which is close to but less than 1.0. For example, the target correlation can be 0.9. This implies that the spatial pattern of the fused precipitation data field at the finer resolution is roughly 90% consistent with the fused precipitation data field at the coarser resolution while the 10% differences are due to the variations associated with the details of the fused data at the finer resolution compared to the fused data at the coarser resolution. In this way, one can basically use the correlation measure to gauge the consistency among the fused precipitation data sets at two different spatial scales, i.e., at the fine and coarse resolutions.

The MKS algorithm is a smoother by nature. If parameters are not well estimated, there is a risk that the fused precipitation data are over smoothed. Once the oversmoothing happens, the maximum values of the

fused precipitation would be significantly smaller than those without being oversmoothed. Meanwhile, the information content of precipitation data will be partially lost. Thus it is important to avoid such oversmoothing from happening. Two approaches are proposed within the MO framework: one approach is to maximize the largest values of fused precipitation data at all of output scales; and the other is to maximize the Shannon information entropy of the fused precipitation data at all output scales. Advantages and disadvantages of these two approaches are discussed and illustrated in section 4.

Based on the discussions above, we propose to improve the estimation of the MKS parameters by formulating it as a multiobjective optimization problem, in which we introduce two groups of objective functions. The first group includes a number of spatial correlations as measures of consistency among the fused precipitation data at the output scales. The second group includes a number of maximization functions of either the largest value or the information entropy of the fused precipitation data at the output scales. In the following, specific objective functions are given for a simple case with two precipitation data sources. For notational convenience, we specify X to represent precipitation data; superscript – and + to represent, respectively, before and after the data fusion; subscript c and f to represent, respectively, a coarse and a fine resolution; $c \rightarrow f$ to represent disaggregation from a coarse resolution to a fine resolution and $f \rightarrow c$ to represent aggregation from a fine resolution to a coarse resolution. Estimation of the MKS parameters can be achieved via maximizing the following four objective functions if maximization of the largest value of the fused precipitation data field is used:

$$g_1(\theta) = Corr\left(X_c^+, X_{f\rightarrow c}^+\right) \tag{5}$$

$$g_2(\theta) = -\left|Corr\left(X_f^+, X_{c\rightarrow f}^+\right) - \rho\right| \tag{6}$$

$$g_3(\theta) = \max\left(X_c^+\right) \tag{7}$$

$$g_4(\theta) = \max\left(X_f^+\right) \tag{8}$$

in which, $g_1(\theta)$ measures the consistency of the fused precipitation data at the coarse resolution; $g_2(\theta)$ measures the consistency of the fused precipitation data at the fine resolution, ρ is a slack parameter to relax the consistency requirement at the finer resolution; $g_3(\theta)$ and $g_4(\theta)$ are the maximum values of the fused precipitation data at the coarse and the fine resolutions, respectively. The slack parameter, ρ, is added to avoid oversmoothing at the finer resolution. Theoretically speaking, the fused data at a fine resolution are able to keep more details of the precipitation field than those at coarser spatial resolutions. If the fused data at a fine resolution are aggregated into a coarser resolution, the aggregated data would be exactly the same as the fused precipitation data at the coarser resolution. If, however, the fused precipitation data at a coarse resolution are disaggregated into a finer resolution, the disaggregated data cannot be the same as the fused data at the finer resolution. The correlation between the disaggregated data and the fused data at the finer resolution will be less than 1.0 even under a theoretical condition. Therefore, the slack parameter, ρ, is needed in equation (6).

If maximization of information entropy is used, $g_3(\theta)$ and $g_4(\theta)$ will be replaced with $g_5(\theta)$ and $g_6(\theta)$ as shown below:

$$g_5(\theta) = -\sum_{i=1}^{n} p(x_{c,i}^+) \log p(x_{c,i}^+) \tag{9}$$

$$g_6(\theta) = -\sum_{i=1}^{n} p(x_{f,i}^+) \log p(x_{f,i}^+) \tag{10}$$

where n is the number of precipitation bins and i is the index of precipitation bin. In this study, precipitation values are divided into equal bins with a bin size of 0.1 mm.

The multiobjective optimization problem formulated with equations (5)–(8) (or (9) and (10)) can be solved in many ways. In this study, it is solved with a multiobjective particle swarm optimization (MOPSO) algorithm [*Wang*, 2011]. Similar to most multiobjective optimization algorithms, the MOPSO algorithm returns not a single optimal solution but a set of Pareto frontiers. However, only one optimal parameter set is to be used in the precipitation data fusion using the MKS algorithm. Our strategy of selecting the optimal solution from the Pareto frontiers includes two steps: (1) select solutions with the largest $g_1(\theta)+g_2(\theta)$, and (2) find the solution with the largest $g_3(\theta)+g_4(\theta)$ or $g_5(\theta)+g_6(\theta)$ from those identified in step (1). Note that the

solution of our proposed MO framework can be obtained by any multiobjective optimization algorithm, such as the genetic algorithm or the simulated annealing algorithm.

We hypothesize that by applying the MO framework to the four objective functions described by equations (5)–(8), we can not only obtain better MKS parameter estimates, but also these estimates are able to keep the essential strength of those associated with the ML scheme and circumvent, at least to a large extent, the weakness of the ML scheme. This hypothesis is also assessed by adding the likelihood function, i.e., equation (4), as one more objective function in section 4.

4. Evaluations

4.1. Experiment Design

Two types of experiments are designed to evaluate the ML scheme and the proposed MO approach. The first is a Monte Carlo experiment, which demonstrates the limitation of the ML scheme and illustrates the rationality of the proposed MO framework. The second is a comparison experiment, which includes between-group comparisons and in-group comparisons. The effectiveness of the ML scheme and the MO framework is statistically evaluated through between-group comparisons. The two approaches of avoiding oversmoothing are evaluated through the in-group comparisons.

To make the analysis of this study representative of real applications, we select a large study domain (Figure 2), bounded by longitudes (88°W, 84°W) and latitudes (37.75°N, 41.75°N). Enclosing the entire state of Indiana, the domain includes 128 × 128 grids at 1/32° resolution and 32 × 32 grids at 1/8° resolution. The average annual precipitation in this area is about 1,000 mm. Precipitation is relatively evenly distributed throughout a year. Typically, precipitation is steady and of long duration in winter and early spring and short but of high intensity during late spring and summer.

Synthetic noisy precipitation data are used in both types of experiments. It is always a concern as to which error model, e.g., additive error model or multiplicative error model, to employ when describing precipitation errors for generating synthetic precipitation data or perturbing precipitation data. Both additive and multiplicative error models have been reviewed by *Tian et al.* [2013]. The MKS smoother usually works with additive errors following a Gaussian distribution due to the nature of Kalman smoother. However, the errors of precipitation measurements from a single instrument, such as radar, are typically described by multiplicative error models. In other words, the multiplicative errors follow the lognormal distribution and not the Gaussian distribution. For such a situation, the multiplicative errors need to be transformed into the additive Gaussian errors by taking a logarithm operation to all precipitation amounts so that the MKS algorithm can be applied. After data fusion, the fused values need to be transformed back into the precipitation amounts by taking an exponentiation operation. Most of the precipitation data products, such as NLDAS 0.125° precipitation, are derived from multiple measurements. NLDAS precipitation combines measurements of NEXRAD Stage II, CPC daily rain gauge and even weather satellite through a sophisticated processing logic. In such a case, it becomes a bit difficult to determine the statistical distribution of the errors for such a composite data product. Unless a thorough investigation is conducted based on a high-density ground network measurements, assuming an additive error model is a

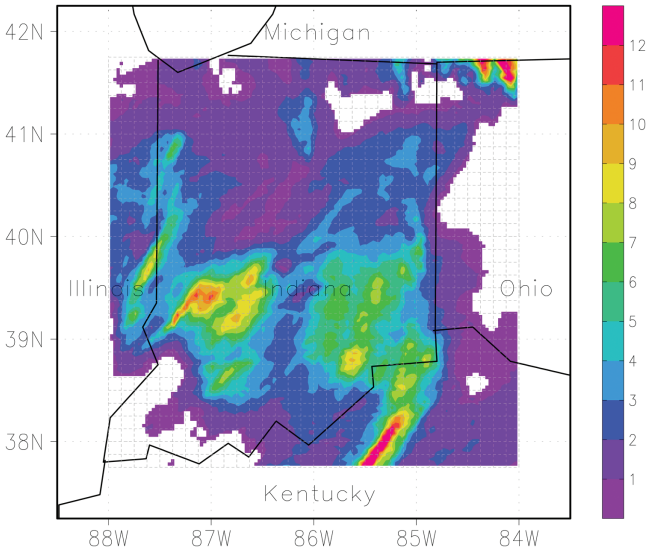

Figure 2. Map of experiment domain. Gray mesh represents 32 × 32 grids at 1/8° resolution. This map illustrates the NEXRAD MPE precipitation data at 09Z 22 September 2003, which are used as the true data in the Monte Carlo experiment in section 4.2. The unit of precipitation data is mm/h.

reasonable starting point for fusing multiple precipitation data products. Such an assumption may introduce suboptimal instead of optimal results. However, choice of the error model is only one of the many potential factors affecting the optimality of the precipitation data fusion results in the real world applications. Moreover, even if the precipitation errors do not strictly follow a multiplicative error model nor an additive error model, the additive error model associated with the MKS algorithm can still be employed to conduct the data fusion since one can always transform a non-Gaussian distribution to a Gaussian distribution before applying the MKS algorithm.

In this study, both the additive and multiplicative error models are used in evaluating the performances of the ML scheme and MO schemes. Synthetic noisy data are generated based on a set of hourly NEXRAD MPE precipitation data. The generated noises are added or multiplied to the MPE precipitation data. The MPE data, which are at a spatial resolution of 4 km and in a specific data format, namely XMRG, are projected into the longitude-latitude coordinate system and resampled into 1/32° and 1/8° resolutions, respectively. In the experiments using the additive error model, the noises are generated based on the Gaussian distributions with zero mean and different standard deviations that are prescribed according to the MPE data. In the experiments using the multiplicative error model, errors are generated based on the lognormal distribution with mean of 1.0 and standard deviation related to the mean and the standard deviation of the MPE data.

In the experiments with the additive error model, the standard deviations are set to be proportional to the standard deviations of the MPE data. For example, at hour k one has the MPE precipitation data (i.e., assumed to be the true data) X_k of a two-dimensional (2-D) field based on which one can calculate the standard deviation of X_k, denoted as s_k. Then, white noises can be sampled from the Gaussian distributions of $\mathcal{N}(0, n_i s_k)$, where n_i, called noise level hereafter, is a multiple of s_k that controls the level of perturbation. The sampled values (i.e., the noises) from $\mathcal{N}(0, n_i s_k)$ are then added to X_k to obtain the synthetically generated noisy precipitation data sets that correspond to different noisy levels. If $n_i = 1$, the standard deviation of added noises is actually the same as the standard deviation of the real MPE precipitation data of the k^{th} hour. Notice that the synthetically generated precipitation value may be negative if the generated white noise has a large negative value. In such a situation, a new value of the white noise will be generated until the synthetic precipitation value is no longer negative. In other words, the noises generated are from truncated Gaussian distributions. This adaptive approach brings three favorable features to the synthetic precipitation data sets. First, the magnitudes of generated data are guaranteed to be nonnegative, which is essential to describe precipitation. Second, the added noises are generated based on normal distribution but not strictly normally distributed due to the noise regeneration procedure. Third, it is easy to control the magnitudes of the noises by adjusting the noise level, i.e., n_i. For details of this synthetic data generation method and the properties of its generated precipitation data, readers are referred to the work by *Wang et al*. [2011].

It is straightforward to generate synthetic precipitation data with the multiplicative errors. Magnitudes of the random multiplicative errors are related to the mean and the standard deviation of precipitation field within the experiment domain (denoted as μ_0 and σ_0 respectively). The synthesized precipitation $x^- = x_0 \cdot \exp(\epsilon)$, in which x_0 is the MPE precipitation and ϵ is a random number following $\mathcal{N}\left(0, \alpha \cdot \frac{\sigma_0}{\mu_0}\right)$. In the formulation with the multiplicative errors, i.e., $\exp(\epsilon)$, α is an adjustable factor that controls the magnitude of errors. In this study, it is set to 0.5.

We use synthetic precipitation data sets to evaluate the MO schemes and the ML scheme mainly to take the advantage of being able to control magnitudes of the errors/noises in the generated precipitation data sets. The approach of using synthetic data has been widely used in data assimilation study for the convenience of performance evaluation [e.g., *Walker and Houser*, 2004].

In all experiments, we apply the MKS algorithm to fuse one set of precipitation data at a coarse resolution, i.e., 1/8°, with the other set of precipitation data at a fine resolution, i.e., 1/32°. Based on the NEXRAD MPE precipitation data, we have two sets of the synthetic precipitation data generated for an entire year of 2003 at both the coarse (1/8°) and the fine (1/32°) resolutions. There is a total number of 2246 precipitation events/fields/images in each set of the synthetic data. As illustrated in Figure 1, the input data have to be organized in a multiscale tree before applying the MKS algorithm. The total number of spatial scales in such a multiscale tree depends on the size of the study domain and the spatial resolutions of the input data. In

this study, the multiscale tree has 8 scales indexing from 0 to 7. Resolutions of 1/8° and 1/32° correspond to, respectively, scales 5 and 7 of the multiscale tree. Therefore, we also call the data at 1/8° and 1/32° resolutions as scale 5 data and scale 7 data, respectively.

In this study, three series of synthetic precipitation data sets at scale 5 are generated with the noise levels of n_5=1.0, 2.0, and 3.0 and four series of synthetic precipitation data sets at scale 7 are generated with the noise levels of n_7=1.0, 2.0, 3.0 and 4.0. Each data series includes 2246 synthetic hourly precipitation fields over the study domain. There is one more noise level employed at scale 7 to describe the reality that precipitation data at finer resolutions may be noisier than those at coarser resolutions. It is worth mentioning that only noises not biases are introduced to the synthetic precipitation data sets. This is because our MKS algorithm [*Parada and Liang*, 2004] can effectively remove the biases as illustrated in the study by *Wang et al*. [2011].

The goal of the multiscale precipitation data fusion is to improve the spatial pattern and the magnitude of precipitation data fields at multiple scales. To evaluate whether such a goal is achieved, we use $\Delta Corr_s = Corr(X_s^{true}, X_s^+) - Corr(X_s^{true}, X_s^-)$ and $\Delta RMSE_s = RMSE(X_s^{true}, X_s^-) - RMSE(X_s^{true}, X_s^+)$ as the metrics at scale s, where X_s^{true} represents the true precipitation amounts, X_s^- represents the synthetically generated precipitation values, and X_s^+ represents the fused precipitation values. $Corr(X_s^{true}, X_s^-)$ and $Corr(X_s^{true}, X_s^+)$ are also expressed as $Corr_s^-$ and $Corr_s^+$ for short. Similarly, $RMSE(X_s^{true}, X_s^-)$ and $RMSE(X_s^{true}, X_s^+)$ are expressed as $RMSE_s^-$ and $RMSE_s^+$ for short as well. The effectiveness of the ML scheme and the MO schemes is evaluated using $\Delta Corr$ and $\Delta RMSE$. If a parameter estimation scheme helps resulting in a larger $\Delta Corr$, it means that this scheme is better than the other schemes for improving the spatial pattern of the precipitation data. Similarly, if a parameter estimation scheme helps resulting in a larger $\Delta RMSE$, it means this scheme is better than the other scheme for improving the magnitudes of the precipitation data.

To facilitate the discussion, we use box plots to illustrate most of experiment results obtained. Box plots graphically depict distributions of samples with the lower (25^{th}) quartile, median, the upper (75^{th}) quartile, 1.5 IQR (interquartile range) of the lower quartile, and 1.5 IQR of the upper quartile. If the samples approximately follow a normal distribution, over 99% of them would fall within the upper and the lower whiskers shown between the 1.5 IQRs of the lower quartile and the upper quartile. In addition, box plots also mark the mean value of each statistical variable, which is used in the result analysis for the comparison experiments in section 4.3. Figure 3 shows the box plots for correlation (vertical axes) in the two upper plots and RMSE (vertical axes) in the two lower plots, which are obtained between the 2246 true and synthetic precipitation fields of 2003. The horizontal axes in Figure 3 represent the values taken for n_5 and n_7, respectively. From Figure 3, one can see, as expected, that the correlation (RMSE) decreases (increases) as the variance increases for both scales 5 and 7, respectively. Figure 3 provides a benchmark as both the MO framework and the ML scheme are expected to generate higher *Corr* and lower *RMSE*, respectively, at scale 5 and scale 7 than the ones shown in Figure 3.

4.2. Monte Carlo Experiment

Monte Carlo experiments are designed to examine the effectiveness of the ML scheme in the multiscale precipitation data fusion process using the MKS algorithm. Based on the results of the Monte Carlo experiment, one can see the weakness of the ideal/theoretical ML scheme when it is applied to real-world problems, in which assumptions and conditions required by the ML scheme and the MKS algorithm are not fully met. Through the Monte Carlo experiment results, one can also see the rationale in developing the MO framework for the MKS algorithm.

The Monte Carlo experiment includes three steps: (1) generate a large amount of parameter sets in their feasible space, (2) conduct data fusion with the generated parameter sets, and (3) compute the corresponding log-likelihood, $Corr_s^+$ and $RMSE_s^+$. As described in section 2.2, the ML scheme identifies parameters for the MKS algorithm by maximizing the log-likelihood function (i.e., equation (4)). If all the requirements/conditions are met, the ML scheme can find the global optimal parameter estimations for the MKS algorithm used. Thus, $Corr_s^+$ (s=5 and 7) should reach its maximum and $RMSE_s^+$ should reach its minimum when the log-likelihood reaches its maximum.

Only one representative precipitation event is selected for conducting the Monte Carlo experiment. Occurred at 09Z 22 September 2003, the precipitation event was a summer storm and covered about 95%

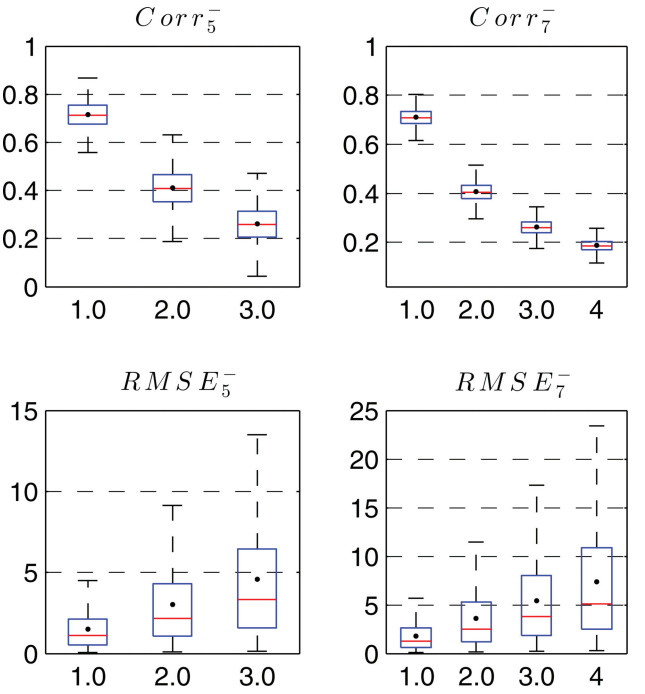

Figure 3. Box plots of the correlation and RMSE between the true and the synthetic precipitation data in 2003. The horizontal axes of subplots $Corr_5^-$ and $RMSE_5^-$ are the noise levels at scale 5, i.e., x_5; the horizontal axes of subplots $Corr_7^-$ and $RMSE_7^-$ are noise level at scale 7, i.e., x_7. For each box, the bottom and the top represent the lower (25th) quartile and the upper (75th) quartile, the lower and the upper whiskers represent 1.5 IQR (interquartile range) of the lower quartile and 1.5 IQR of the upper quartile, and the black dot represents the mean of *Corr* or *RMSE*.

area of the experiment domain shown in Figure 2. In the Monte Carlo experiment, the noise levels, i.e., n_5 and n_7, are set to 2.0 when generating the synthetic precipitation data at both scales 5 and 7. We randomly sample 1,000,000 parameter sets, including $\Sigma(0)$, $Q(s)$ (s=1, 2, . . ., 7), and $R(s)$ (s=5 and 7) using a uniform distribution. Since all parameters are essentially error variances of precipitation data, the feasible range is set to [0.1, 10.0] for each of them. After fusing the precipitation data at scales 5 and 7 with all sampled parameters using the MKS algorithm, we compute the log-likelihood, $Corr_5^+$, $Corr_7^+$, $RMSE_5^-$ and $RMSE_7^+$ corresponding to each parameter set.

The effectiveness of the ML scheme is examined based on the relationships between the log-likelihood and $Corr_5^+$, $Corr_7^+$, $RMSE_5^+$, and $RMSE_7^+$ respectively, which are shown in the scatter plots of Figure 4. An essential finding from Figure 4 is that the ML scheme has different effectiveness at scale 5 and scale 7. First, it is much more effective at scale 5 than at scale 7. Both $Corr_5^+$ and $RMSE_5^+$ converge to their maximum and minimum values, respectively, when the log-likelihood approaches its maximum. As an objective function, the log-likelihood defined in equation (4) appears to be consistent to the correlation and RMSE at the coarser resolution in the Monte Carlo experiment. This provides an affirmation that the ML scheme is more likely to produce parameter estimates for the MKS algorithm that are in favor of the fused precipitation data products at coarser resolutions.

On the other hand, the ML scheme is not guaranteed to result in parameter estimates which are also effective for the fused data at scale 7. That is, local optima rather than global optima are likely obtained by the ML scheme in this case. As shown in Figure 4, $Corr_7^+$ may converge to two substantially different extreme values when the log-likelihood approaches its maximum. One extreme value is close to the upper bound of $Corr_7^+$ while the other is close to the lower bound of $Corr_7^+$ (see Figure 4). Similar situation also occurs to *RMSE* as shown in Figure 4. If $Corr_7^+$ goes to its lower extreme value or $RMSE_7^+$ goes to its upper extreme value, there will be no gain through data fusion in terms of improving the spatial patterns and magnitudes of the precipitation data fields at scale 7. This example clearly indicates that the estimated parameters using the ML scheme may not work at finer resolutions due to the combined effects of encountering local maxima and the required conditions for the algorithm being not fully met in the real-world applications.

Nevertheless, there are no monotonous relationships between the log-likelihood and $Corr_s^+$ or $RMSE_s^+$ for s=5 and 7. An increase of the log-likelihood does not necessarily mean an increase of $Corr_s^+$ or a decrease of $RMSE_s^+$. In the ML scheme used, the log-likelihood is maximized using the EM algorithm, which usually stops iterating when the log-likelihood reaches a local maximum or after a given number of iterations is reached. This example clearly illustrates the limitations of the ML scheme.

Findings from the Monte Carlo experiments are consistent with the results shown in *Wang et al*. [2011], where improvements at a coarser resolution are found to be much more significant than those at a finer resolution. The maximization of the log-likelihood is neither a necessary nor a sufficient condition for achieving improvements at finer resolutions. If one wants to achieve improvements at multiple scales,

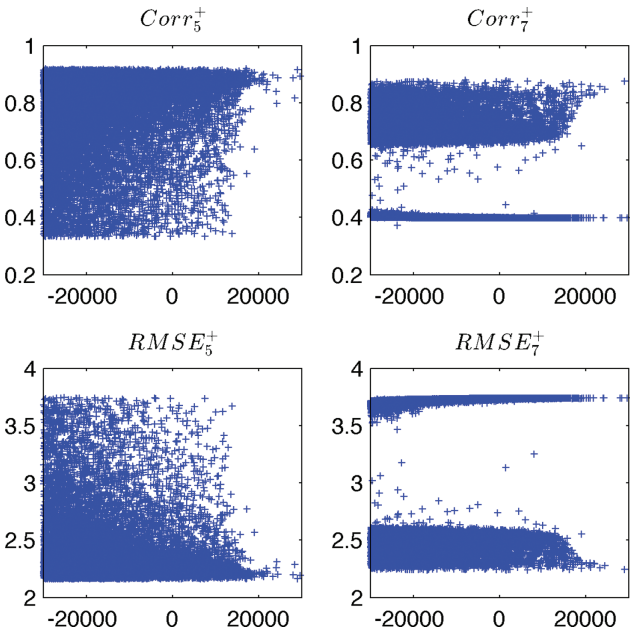

Figure 4. Scatter plots of log-likelihood and $Corr_5^+$, log-likelihood and $Corr_7^+$, log-likelihood and $RMSE_5^+$, and log-likelihood and $RMSE_7^+$. The horizontal axes of all subplots are log-likelihood.

especially at finer resolutions, there is a critical need to develop a new scheme to estimate the parameters of the MKS algorithm.

4.3. Comparison Experiments

4.3.1. Experiments With Additive Errors

A series of comparison experiments are designed to illustrate the strength and limitations of the proposed MO schemes as opposed to the ML scheme. Twelve scenarios of the multiscale precipitation data fusion cases have been constructed by combining the noisy precipitation data at a fine resolution with those at a coarser resolution. As described in section 4.1, we have generated the synthetic noisy precipitation data at the coarse resolution (i.e., 1/8°) with three noise levels (i.e., n_5=1.0, 2.0 and 3.0) and the synthetic noisy precipitation data at the fine resolution (i.e., 1/32°) with four noise levels (i.e., n_7=1.0, 2.0, 3.0 and 4.0). These synthetic precipitation data thus form 12 (i.e., 3 × 4) combinations for conducting the MKS data fusion exercises. For example, the combination of n_5=2.0 with n_7=4.0 indicates a scenario in which a set of noisy precipitation data at 1/8° resolution is fused with much noisier data at 1/32° resolution. In this particular example, the data noisy level at the fine resolution is about two times of that at the coarser resolution. Generally speaking, if $n_5 > n_7$, it means that the combination mimics a scenario in which the coarse resolution data are fused with less noisy data at a finer resolution. On the other hand, if $n_5 < n_7$, it means a scenario in which the fine resolution data are fused with less noisy data at a coarser resolution. If $n_5 = n_7$, it means a scenario in which the coarse resolution data is fused with the finer resolution data that have similar or comparable level of noises. Since the precipitation data at fine resolutions are usually noisier than those at coarser resolutions in the real world, the maximum value of n_7 (i.e., 4.0) is thus greater than that of n_5 (i.e., 3.0).

Each of the 12 scenarios has two series of the synthetic precipitation data, one at 1/32° and the other at 1/8° resolutions, for data fusion. Each series includes 2246 noisy precipitation fields for year 2003 in the study domain. The two series of data are fused field by field using the MKS algorithm. The ML scheme is firstly used to estimate the parameters. Fused precipitation data with the ML scheme, notated with number 0 hereafter, are used as references to evaluate the MO framework with three approaches that are designed to avoid the over smoothing problem. Equations (5) and (6) are the core part of the MO framework. No matter which approach is used, they are part of the objective functions. The first approach uses equations (7) and (8) to maximize the maximum values of the fused precipitation data (#1 MO scheme); the second approach uses the likelihood function (equation (4)) in addition to equations (7) and (8) (#2 MO scheme); and the third approach uses equations (9) and (10) to maximize the information contents of the fused precipitation data at the output resolutions (#3 MO scheme). For notational convenience, the MO schemes with the three approaches are marked with number 1, 2, and 3 in the result plots and analyses.

Even though the fused precipitation data sets at any resolution, i.e., from the finest to the coarsest scale of the multiscale tree (see Figure 1), can be output with the MKS algorithm, we just output the fused precipitation data sets at the 1/8° and 1/32° resolutions to evaluate the effectiveness of the MO framework versus the ML scheme since the true values (assumed) are available at these two scales. For each scenario, we compute $\Delta Corr_s$ and $\Delta RMSE$ (s = 5, 7) for all of the 2246 precipitation fields (i.e., precipitation images) for schemes 0, 1, 2, and 3. We then compare the statistics (e.g., mean, quartiles) of $\Delta Corr_s$ and $\Delta RMSE_s$, instead of the $\Delta Corr_s$ and $\Delta RMSE_s$ for individual precipitation fields among schemes 0, 1, 2, and 3. The large number

of samples, i.e., 2246, included in the analyses guaranties the statistical significance of our comparison studies. Thus, the overall performances of each individual scheme (i.e., the MO and ML schemes) can be more objectively evaluated.

Figure 5 shows the box plots of $\Delta Corr_s$ ($s = 5, 7$) for the 12 scenarios. Each of them has results obtained with the ML scheme and the three MO schemes. In Figure 5, if a MO scheme leads to a larger mean of $\Delta Corr_s$, it indicates that the MO scheme statistically performs better than the ML scheme on average based on the 2246 precipitation fields investigated. Similarly, if a MO schemes results in a larger value of median, it indicates that the MO scheme performs better than the ML scheme over half of the 2246 precipitation fields for the given combination of n_5 and n_7. Otherwise, it indicates that the ML scheme performs better than the MO scheme.

In Figure 5, the differences of $\Delta Corr_5$ between results of the ML scheme and the MO schemes are relatively small for the 12 scenarios compared with the corresponding differences of $\Delta Corr_7$. In terms of the $\Delta Corr_5$ values, the MO schemes are better in eight scenarios, while the ML scheme is better in 4 scenarios in which the noise levels at the finer resolution are higher or much higher than those at the coarser resolution. These four scenarios are ($n_5 = 1, n_7 = 2$), ($n_5 = 1, n_7 = 3$), ($n_5 = 1, n_7 = 4$), and ($n_5 = 2, n_7 = 4$). Such results indicate that the MO schemes are slightly underperformed than the ML scheme on improving the spatial pattern of the coarser precipitation data when the coarser precipitation data have better or much better quality than the finer precipitation data. For the results of scenarios in which $n_5 \geq n_7$, the MO schemes produce larger values of the mean and the median of $\Delta Corr_5$ than those of the ML scheme. This indicates that the MO schemes perform better than the ML scheme in terms of improving the spatial patterns of the precipitation data at coarser resolution when the precipitation data at the coarser resolution have poorer quality than those at the finer resolution. In addition, the box plots in Figure 5 reveal that the improvements with the MO schemes are greater than those with the ML scheme when the coarser precipitation data have much poorer quality than the finer precipitation data.

In Figure 5, it can also be observed that the three MO schemes perform closely in terms of improving $\Delta Corr_5$. For most of the scenarios, the #2 MO scheme performs slightly better than the #1 MO scheme and the #3 MO scheme performs slightly better than the #2 MO scheme in terms of the mean, the median, the upper quartile and the lower quartile. However, the performance differences are very small. Comparing to the #1 MO scheme, the computational time of the #2 MO scheme is almost doubled because the log-likelihood function is added as an extra objective function. The gain of the #2 MO scheme over the #1 MO scheme is almost negligible. This implies that the 4 objective functions of the #1 MO scheme include most of the information which could be introduced by the log-likelihood function (i.e., equation (4)) for the purpose of improving precipitation data at a coarser resolution. The #3 MO scheme also almost doubles the computation time of the #1 MO scheme, because computing information entropy of equations (9) and (10) takes much longer time than finding the maximum precipitation values (equations (7) and (8)). Even though the gain of the #3 MO scheme is also minor at the coarse resolution compared to the #1 MO scheme, the gain at the finer resolution is more pronounced as can be seen in Figure 5.

For the fused precipitation at the finer resolution, i.e., 1/32° (scale 7), Figure 5 shows that the MO schemes perform better or much better than the ML scheme on improving the spatial patterns of the fused precipitation at this resolution for all of the 12 scenarios. It does not matter which situations of the data quality are at the coarse and fine resolutions, i.e., either $n_5 > n_7$, $n_5 = n_7$ or $n_5 < n7$, the mean, the lower and upper quartiles, the median, and the two whiskers of $\Delta Corr_7$ of the three MO schemes are always significantly higher than those of the ML scheme. Specifically, all lower quartiles of $\Delta Corr_7$ of the three MO schemes are larger than the upper whiskers of the corresponding $\Delta Corr_7$ of the ML scheme when $n_5 > = n_7$. This indicates that the MO schemes perform better than the ML scheme for at least 75% of the 2246 precipitation fields. When $n_5 < n_7$, all of the lower whiskers of $\Delta Corr_7$ of the MO schemes are larger than the lower whiskers of corresponding $\Delta Corr_7$ of the ML scheme, which indicates that the MO schemes perform better than the ML scheme for at least 90% of the 2246 precipitation fields. This performance of the MO schemes over the ML scheme becomes even much better when the precipitation data at the finer resolution are noisier. Although the MO schemes perform slightly worse in 4 scenarios (out of 12 scenarios) than the ML scheme at the coarser resolution, the fused precipitation data at the coarser resolution with the ML scale are already quite good as shown in the work of *Wang et al*. [2011]. Thus, the slight under-performance by the MO schemes at the coarser resolution is not a cause for concern. Overall, the the MO schemes are promising for their good performance.

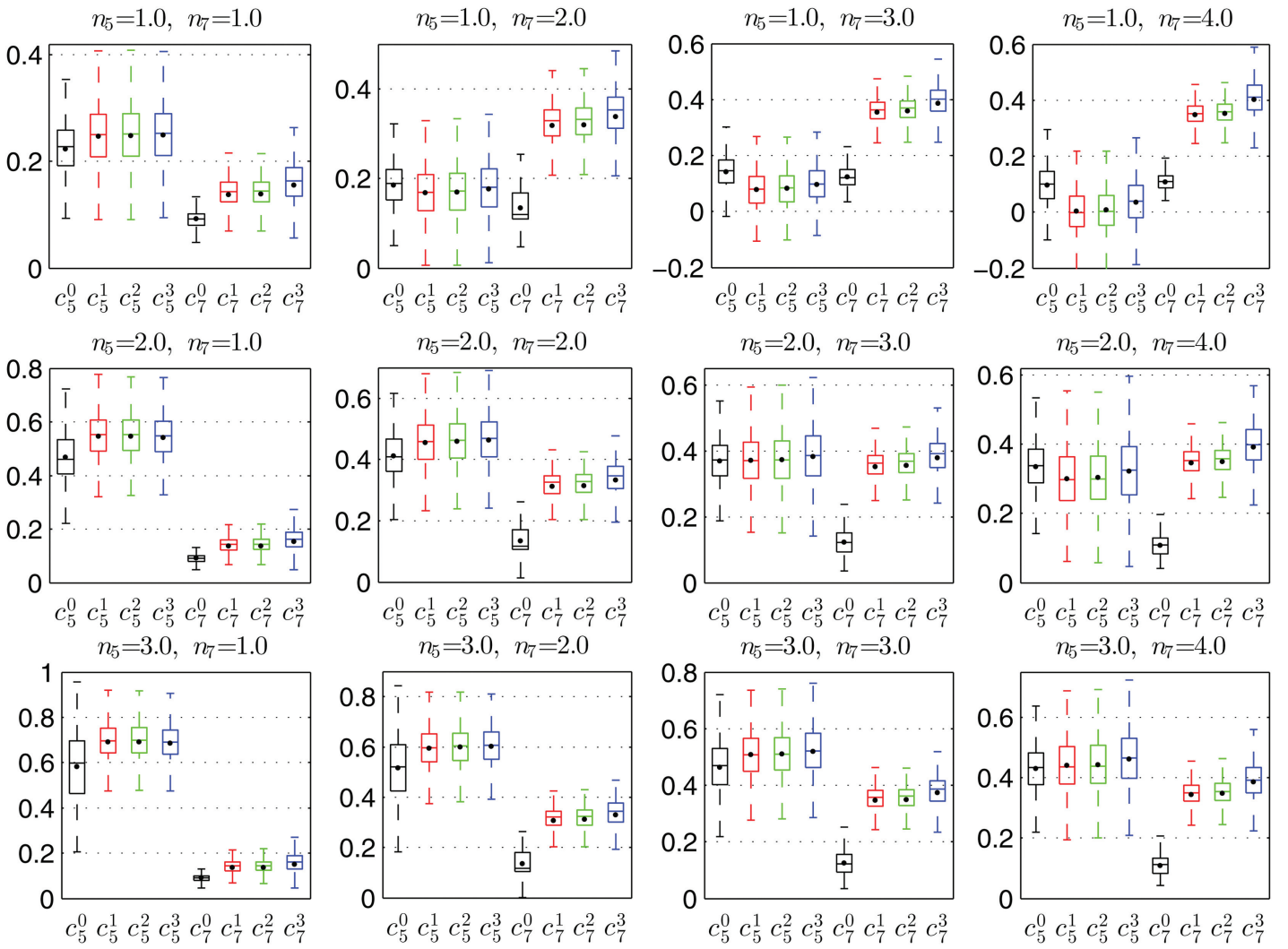

Figure 5. Box plots of $\Delta Corr_5$ and $\Delta Corr_7$ for the precipitaiton results with the ML scheme (in black color) and the MO schemes (in red, green, and blue colors) for the 12 scenarios with the additive error model. In the labels of the horizontal axes of all subplots, C denotes $\Delta Corr$ and the supper scripts 0, 1, 2, and 3 denote the ML scheme and the MO schemes. The title of each subplot describes the combination of noise levels at scale 5 and scale 7 of the scenario. Descriptions of symbols are the same as those in Figure 3.

The three MO schemes perform differently in terms of improving the spatial patterns of the precipitation data at the finer resolution. For most of the scenarios, the mean, median, upper quartile and lower quartile of the $\Delta Corr_7$ of the #3 MO scheme are clearly larger than the corresponding ones of the #1 and the #2 MO schemes. The #2 MO scheme performs slightly better than or the same as the #1 MO scheme. This implies again that the log-likelihood function (i.e., equation (4)) included in the #2 MO scheme does not bring any significant gain to the fused precipitation data. That is, the effect of the likelihood function is indirectly represented by those of equations (5)–(8). However, the information entropy represented by equations (9) and (10) does bring in more information than that by equations (7) and (8) at a cost of doubling the computational time.

Results of $\Delta Corr_7$ of the ML scheme and the MO schemes for each scenario are also evaluated using statistical hypothesis tests. Based on the Q-Q plot (figures not shown), we find that none of the distributions of $\Delta Corr_7$ follow the normal distribution. Therefore, we use the Kolmogorov-Smirnov test to examine the differences of $\Delta Corr_7$ between the ML scheme and the MO schemes and check whether they are significantly different. Unlike the paired t-test, which only works well with normal distributions, the Kolmogorov-Smirnov test can be used for cases following any type of continuous distributions. The null hypothesis is that the differences are not significant and the alternative hypothesis is that the differences are significant.

Results of the Kolmogorov-Smirnov test (at 1% significant level) show that the distribution differences of $\Delta Corr_7$ between the MO schemes and the ML scheme are significant for all of the 12 scenarios shown in Figure 5. These results confirm again the significantly better performances of the MO schemes at the finer resolution. Therefore, we can infer that the MO schemes are significantly better than the ML scheme in deriving fused precipitation data at finer resolutions in terms of improving the spatial patterns of the precipitation. The #1 MO scheme is a better choice for limited computational resources and the #3 MO scheme is a better choice when computational resources are sufficient.

Figure 6 shows the box plots of $\Delta RMSE_s$ ($s = 5, 7$) for the 12 scenarios. Like Figure 5, each scenario represents the fused precipitation data using the MKS algorithm with the ML scheme and the three MO schemes. In Figure 6, if the MO schemes lead to larger values of $\Delta RMSE_s$, it indicates that statistically, the MO schemes perform better than the ML scheme. Otherwise, the MO schemes are statistically not as good as the ML scheme. In addition, if any of the MO schemes results in higher values of $\Delta RMSE_s$, it means that the MO scheme has a better choice of the objective functions in terms of improving the magnitudes of fused precipitation data.

In Figure 6, the differences of $\Delta RMSE_5$ between the ML scheme and the MO schemes are relatively small for all of the 12 scenarios compared to the corresponding differences of $\Delta RMSE_7$. Which scheme performs better also depends on the noise levels at both scales. Specifically, the performance of the MO schemes is slightly better than that of the ML scheme when $n_5 > n_7$, i.e., for the combinations of $n_5 = 2.0$ and $n_7 = 1.0$, $n_5 = 3.0$ and $n_7 = 1.0$, and $n_5 = 3.0$ and $n_7 = 2.0$. This indicates that the MO schemes are better choices than the ML scheme when fusing much noisier precipitation data at a coarser resolution with less noisy data at a finer resolution. When $n_5 \leq n_7$, i.e., when the precipitation data at the fine resolution is noisier than that at the coarser resolution, the performance of the MO schemes is slightly worse than that of the ML scheme. For example, the lower and the upper quartiles and the medians of $\Delta RMSE_5$ of the MO schemes are smaller than those of $\Delta RMSE_5$ of the ML scheme for the scenarios of $n_5 = n_7 = 2.0$ and 3.0, $n_5 = 1.0$ and $n_7 = 2.0$, $n_5 = 1.0$ and $n_7 = 3.0$, $n_5 = 1.0$ and $n_7 = 4.0$, $n_5 = 2.0$ and $n_7 = 3.0$, $n_5 = 2.0$ and $n_7 = 4.0$, and $n_5 = 3.0$ and $n_7 = 4.0$. But most of the differences are very small or negligible. Since the fused precipitation data at the coarser resolution with the ML scheme are already quite good as shown in the work of *Wang et al.* [2011], the smaller values of $\Delta RMSE_5$ with the MO schemes than those with the ML scheme are not a cause for concern. Among the three MO schemes, the #1 and #2 MO schemes perform very closely. This once again shows that the objective functions of #1 MO scheme are sufficient enough and there is no need to add the likelihood function. The #3 MO scheme is slightly better than the #1 and the #2 MO schemes for most of scenarios.

On the other hand, the MO schemes perform much better than the ML scheme on improving the magnitude of the fused precipitation data at the finer resolution. As shown in Figure 6, the lower and upper quartiles, the means and medians of the $\Delta RMSE_7$ of the MO schemes are clearly higher than the corresponding counterparts of the ML scheme for all of the 12 scenarios. The differences between $\Delta RMSE_7$ of the MO schemes and $\Delta RMSE_7$ of the ML scheme are also examined using the Kolmogorov-Smirnov test (at 1% significant level) similar to the correlation cases shown in Figure 5. Again the test results indicate that all of the differences are statistically significant. This implies that the MO schemes are significantly better than the ML scheme in terms of improving the magnitudes of the fused precipitation at the finer spatial resolution using the MKS algorithm. Among the three MO schemes, the #1 and the #2 MO schemes behave similarly while the #3 MO scheme also performs better than the #1 and #2 MO schemes as indicated by its higher values of the lower and the upper quartiles, the mean and the median.

Moreover, the performance of the #3 MO scheme is illustrated with an example having very noisy data. Figure 7 shows a precipitation event before (i.e., X_5^- and X_7^-) and after (i.e., X_5^+ and X_7^+) the precipitation data fusion using the MKS algorithm with the #3 MO scheme. In the figure, the synthetically generated noisy precipitation fields (X_5^- and X_7^-) are for the precipitation event at 09Z 22 September 2003 with $n_5 = 2.0$ and $n_7 = 2.0$. The true precipitation image of this event at scale 7 is shown in Figure 2. Comparing the precipitation field shown in Figure 2 with those of X_5^- and X_7^- shown in Figure 7, the spatial pattern of the true precipitation field has been heavily contaminated in the synthetic precipitation fields at both scales 5 and 7. After the data fusion using the MKS algorithm with the #3 MO scheme, the original spatial pattern can be mostly restored at both scales. However, the fused precipitation data at scale 7 have lost some details at this scale. This is a common drawback of improving precipitation data at a fine resolution with precipitation data from a coarser resolution. It is also partially caused by one of the constraints of the MO schemes, i.e., the one shown in equation (6). A relaxation of equation (6) may reduce the effect of losing details at the finer resolution.

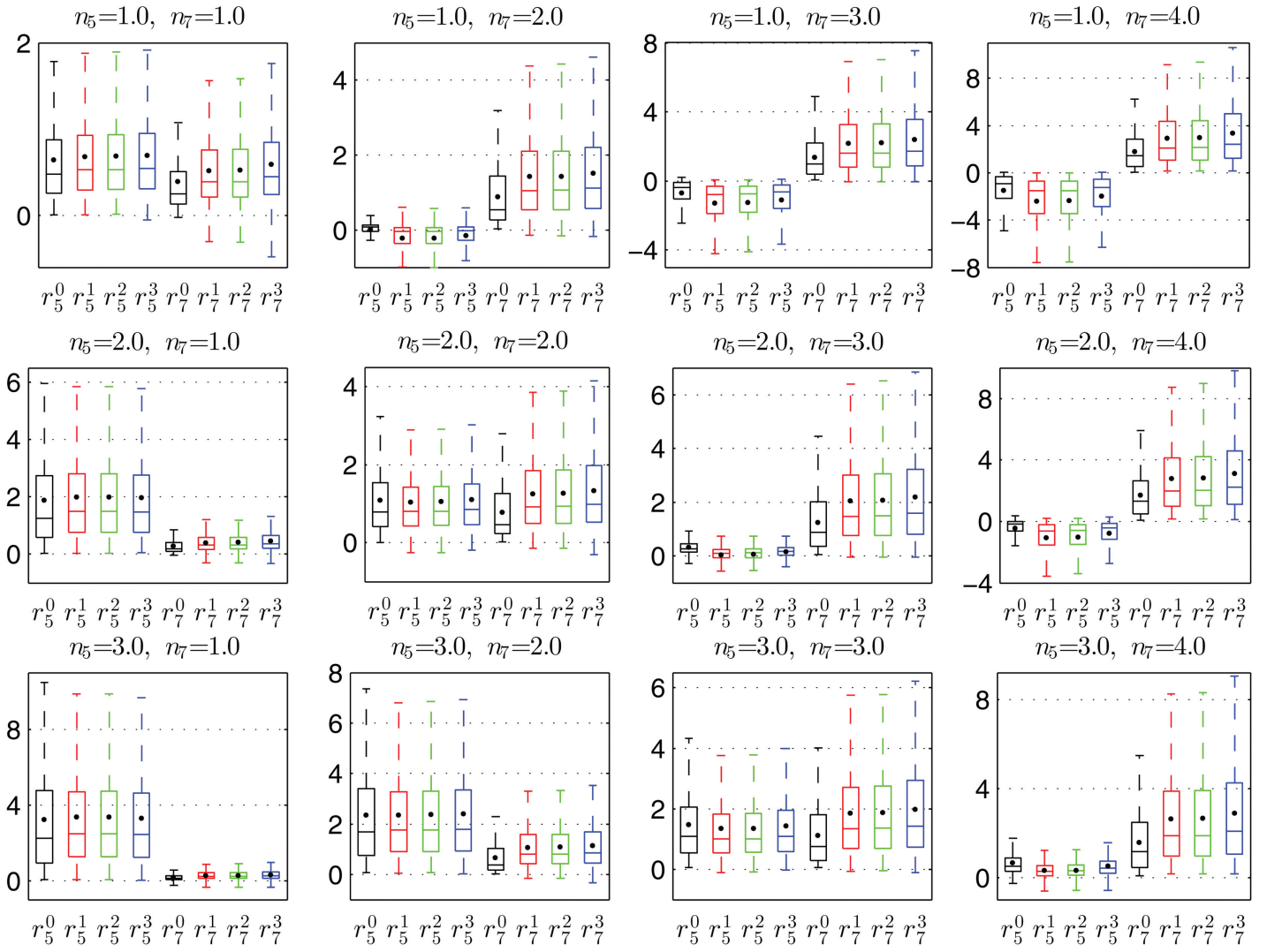

Figure 6. Box plots of $\Delta RMSE_5$ and $\Delta RMSE_7$ for the precipitation data fusion results using the ML scheme and the MO schemes for the 12 scenarios with the additive error model. Descriptions of symbols are similar to those in Figure 5.

4.3.2. Experiment With Multiplicative Errors

In this section, performances of the ML and the MO schemes are investigated with multiplicative errors and compared to the findings obtained with the additive errors as discussed in the previous section (i.e., section 4.3.1). In particular, the #3 MO scheme is used to compare with the results from the ML scheme.

The box plots of $\Delta Corr$ and $\Delta RMSE$ are shown, respectively, in Figure 8 for the ML and the #3 MO schemes at scales 5 and 7. Comparing Figure 8 to Figures 5 and 6, it can be seen that results with the multiplicative error model are similar to those with the additive error model. That is, for the case with the multiplicative errors, the MO scheme also performs slightly better than the ML scheme for the coarse spatial resolution. Specifically, the lower and upper quartiles, and the median of $\Delta Corr$ and $\Delta RMSE$ obtained with the MO scheme are slightly higher than those obtained with the ML scheme at scale 5. The MO scheme performs much better than the ML scheme at the finer spatial resolution, as indicated by the lower and upper quartiles, and the median of $\Delta Corr$ and $\Delta RMSE$. Also, the relative behaviors between the MO scheme and the ML scheme that are associated with the multiplicative error model (see Figure 8) are similar to those with the additive error model as shown in Figures 5 and 6. In other words, Figure 8 clearly shows that the results and findings from this study using the additive error model are general and that they are similar to those using the multiplicative error model.

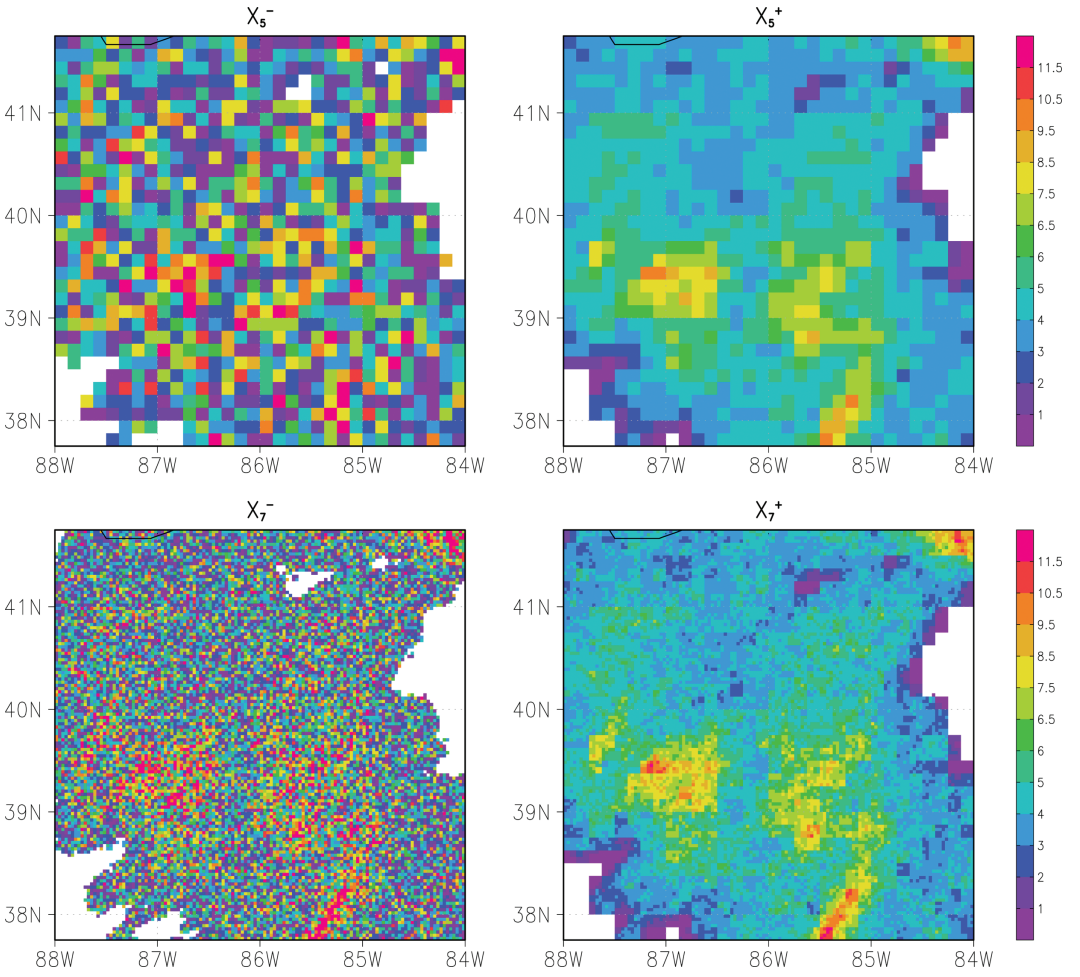

Figure 7. Example of multiscale precipitation data fusion using the MKS algorithm with the MO scheme ($n_5 = 2.0$ and $n_7 = 2.0$) at 09Z 22 September2003. X_5^- and X_5^+ denote synthetic precipitation data and fused precipitation data at 1/8° resolution (scale 5). X_7^- and X_7^+ denote synthetic precipitation data and fused precipitation data at 1/32° resolution (scale 7).

Figure 9 shows the scatter plots between $Corr^-$ and $Corr^+$ and $RMSE^-$ and $RMSE^+$ for scales 5 and 7, respectively, where the multiplicative error model is used. From the scatter plots of $RMSE^-$ and $RMSE^+$ in Figure 9, it can be clearly seen that the MO scheme has better performance than the ML scheme on reducing *RMSE* when the input data have large errors, especially large errors at the finer spatial resolution. When the input data are less noisy, the difference in performance between the two schemes becomes smaller. In addition, Figure 9 provides an overview of how the MO and the ML schemes perform at each of the 2246 individual precipitation fields with varying levels of errors.

5. Conclusions

This paper presents a general multi-objective (MO) parameter estimation framework for the Multiscale Kalman Smoother (MKS) algorithm used for precipitation data fusion. Three parameter estimation schemes have been introduced with the MKS algorithm to avoid over-smoothing of the precipitation data fields. Formulations are established for the three MO parameter estimation schemes based on the enforcement of the objectives of the multiscale precipitation data fusion. The objective functions associated with each of the specific MO schemes have clear physical meanings that are related to the precipitation data. This helps making the fused precipitation data fields meet the expectations at multiple scales. A Monte Carlo experiment has been conducted to investigate the limitations of the maximum likelihood (ML) scheme for the multiscale precipitation data fusion and to justify the rationale in developing the MO schemes, which significantly enhance the performance of MKS at the finer resolutions. The three proposed MO schemes have

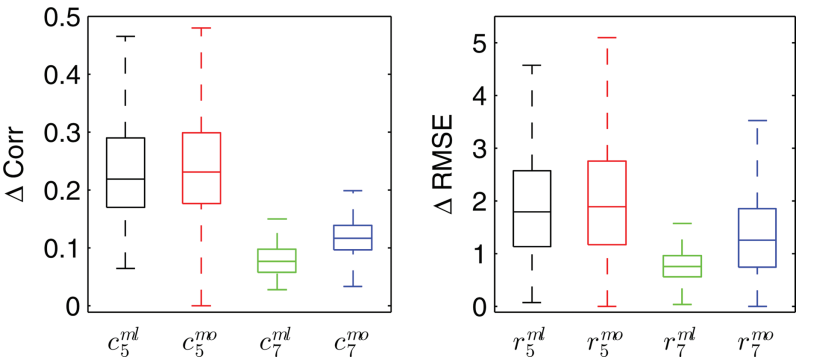

Figure 8. Box plots of Δ*Corr* and Δ*RMSE* for the precipitation data fusion results with the multiplicative error model.

been extensively evaluated against the conventional ML scheme. Altogether 2246 precipitation events/fields from 2003 were evaluated in terms of the improvement regarding the spatial patterns and the magnitudes of the precipitation data based on the results of the 12 scenario experiments.

Results from this study can be summarized in two aspects. First, the limitations of the ML scheme for estimating the parameters of the MKS algorithm have been clearly demonstrated for the real world precipitation data fusion applications. This ML scheme does not work well at fine resolutions even though it is effective at coarser resolutions. At the fine resolution, it is possible that only limited improvements can be achieved on the fused precipitation data fields in their spatial patterns and magnitudes using the MKS algorithm with the ML scheme. The reasons are due to the combination of (1) the assumptions made in the ML scheme are not always met, and (2) local optima instead of global optima are obtained. In order to improve the performance at the fine resolutions, we have developed a multiobjective (MO) parameter estimation framework for the MKS algorithm. In the MO framework, we formulated two core objective functions (i.e., equations (5) and (6)) to simultaneously improve the spatial patterns and the magnitudes of the fused precipitation data fields at multiple scales. Three different schemes have been investigated with the MO framework to reduce oversmoothing of the precipitation details at the fine resolution.

Comparisons between our three new MO schemes and the ML scheme via a large number of precipitation events/fields over a large study domain show that the proposed three MO schemes have significantly better performances on improving the qualities of the fused precipitation data fields at the fine spatial resolution. The improvements brought by the MO schemes are even more significant when the precipitation data at the fine spatial resolutions are much noisier than the precipitation data at the coarser spatial resolutions. At the coarse spatial resolution, if the precipitation data are noisier than the precipitation data at the finer resolution, the new MO schemes also perform better than or comparable to the ML scheme on improving the spatial patterns and the magnitudes of precipitation data fields. Among the three MO schemes, the #1 and the #2 schemes work similarly at both spatial scales.

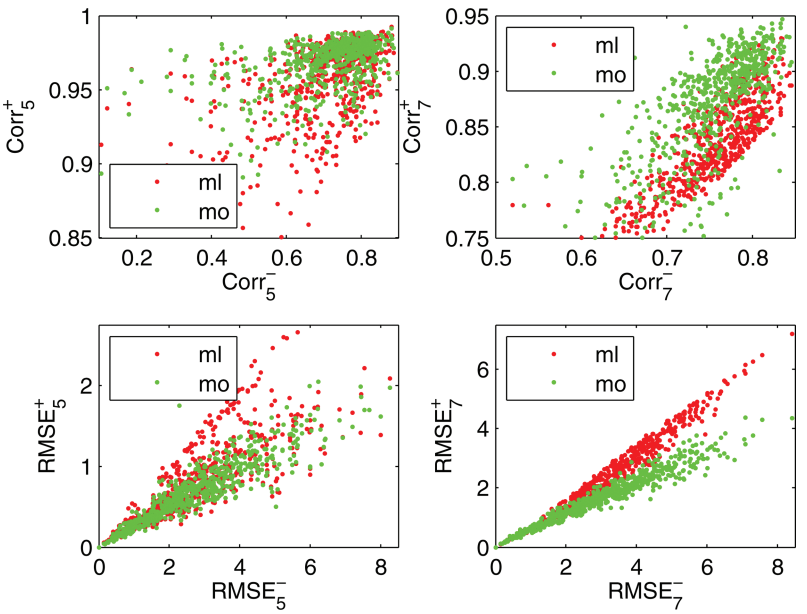

Figure 9. Scatter plots of $Corr^-$ and $Corr^+$ and scatter plots of $RMSE^-$ and $RMSE^+$ at scale 5 and scale 7 for the precipitation data results with the multiplicative error model.

This means that the likelihood function (i.e., equation (4)) could be mostly represented by equations (5)–(8). The #3 scheme results in a better performance of the MKS algorithm than those of the #1 and #2 schemes. This means that the objective functions of the information entropy can bring in more useful information to fused precipitation data than the two objective functions of maximization (i.e., equations (7) and (8)). The #3 MO scheme is a better choice than the #1 MO scheme only if the computational resources are sufficient. Otherwise, the #1 MO scheme is a better choice.

Second, our numerical results have shown that the MO schemes can effectively represent the main features characterized by the ML scheme for the fused precipitation data fields at the fine resolution. In section 4.3, the #2 MO scheme does not show advantages to the #1 MO scheme for most cases. The advantages are, in fact, negligible if any. The #3 MO scheme outperforms the #2 MO scheme generally. This implies that the two objective functions of the information entropy may represent more information than the log-likelihood function. Therefore, results obtained from the #3 MO scheme can be considered to have similar or even more strength than that with the ML scheme.

In summary, the MO parameter estimation framework, in reference to either the #1, #2, or #3 MO scheme, is effective for the MKS algorithm in fusing precipitation data, especially for deriving precipitation data products at finer spatial resolutions. On the other hand, the MO framework takes longer computational time due to its multiobjective optimization nature. Therefore, if the fused precipitation data products are desired at coarser spatial resolutions, the ML scheme is recommended. But if the fused precipitation data are desired at finer spatial resolutions, the MO framework is recommended due to its much better performance at the finer spatial resolutions while its performance at the coarse resolutions is also very good. The concepts and ideas of the proposed MO framework in combining with the MKS algorithm are general, and thus can also be applied, in combination, to other approaches as well.

The main limitation of this study stems from the use of hypothetical experiments with synthetic precipitation data. In the next step of the research, we plan to derive new precipitation data sets based on real data, such as the NLDAS precipitation data and the NEXRAD MPE data. Furthermore, the quality of the derived precipitation data will be evaluated with hydrological models against observations of stream flow, evapotranspiration, and soil moisture contents. For the further development of data fusion algorithm and parameter estimation method, we also plan to combine the Particle Filter (PF) [*Pitt and Shephard*, 1999] with the framework of our MKS algorithm. With many successes in hydrology applications [*Moradkhani et al*., 2005], the PF algorithm could help relaxing the linear assumption on state-space equations and the Gaussian assumptions on error terms in the MKS framework. We plan to combine the PF method with the MKS algorithm and conduct a systematic assessment of such an approach. We also plan to compare it with the approach of transferring the data of non-Gaussian errors to meet the Gaussian error assumption. We will assess the strength and weakness of each approach in terms of the performance and computational cost. In our plan, the state variables and parameters will eventually be estimated simultaneously based on Bayesian inference. If this new method succeeds, choosing error models will no longer be an issue of the precipitation data fusion using the MKS algorithm.

Acknowledgments
The authors are thankful to the Associate Editor and the reviewers for their valuable comments and suggestions. We thank Jeen-Shang Lin for the valuable discussions. We also thank Server Levent Yilmaz for his help in providing computing assistance of using the TeraGrid resources of the Center for Simulation and Modeling at the University of Pittsburgh. This work was partially supported by the NASA grants NNA07CN83A and NNX12AQ25G and by the U.S. Department of Transportation grant OASRTRS-14-H-PIT to the University of Pittsburgh.

References

Bocchiola, D. (2007), Use of scale recursive estimation for assimilation of precipitation data from TRMM (PR and TMI) and NEXRAD, *Adv. Water Resour.*, *30*(11), 2354–2372, doi:10.1016/j.advwatres.2007.05.012.

Chou, K., A. Willsky, and R. Nikoukhah (1994), Multiscale systems, Kalman filters, and Riccati-equations, *IEEE Trans. Autom. Control*, *39*(3), 479–492.

Chou, K. C. (1996), Maximum-likelihood estimation of multiscale stochastic model parameters, in *Proceedings of IEEE-SP International Symposium on Time-Frequency and Time-Scale Analysis*, pp. 17–20, IEEE, Paris, France.

Chou, K. C., and A. S. Willsky (1991), Modeling and estimation of multiscale processes, in *1991 Conference Record of the Twenty-Fifth Asilomar Conference on Signals, Systems and Computers*, vol. 2, pp. 778–784, IEEE, Pacific Grove, Calif.

Cosgrove, B. A., et al. (2003), Real-time and retrospective forcing in the North American Land Data Assimilation System (NLDAS) project, *J. Geophys. Res.*, *108*(D22), 8842, doi:10.1029/2002JD003118.

Digalakis, V., J. R. Rohlicek, and M. Ostendorf (1993), Ml estimation of a stochastic linear system with the EM algorithm and its application to speech recognition, *IEEE Trans. Speech Audio Process.*, *1*(4), 431–442.

Gill, M. K., Y. H. Kaheil, A. Khalil, M. McKee, and L. Bastidas (2006), Multiobjective particle swarm optimization for parameter estimation in hydrology, *Water Resour. Res.*, *42*, W07417, doi:10.1029/2005WR004528.

Gorenburg, I., D. McLaughlin, and D. Entekhabi (2001), Scale-recursive assimilation of precipitation data, *Adv. Water Resour.*, *24*(9-10), 941–953.

Gupta, R., V. Venugopal, and E. Foufoula-Georgiou (2006), A methodology for merging multisensor precipitation estimates based on expectation-maximization and scale-recursive estimation, *J. Geophys. Res.*, *111*, D02102, doi:10.1029/2004JD005568.

Hu, X., and R. Eberhart (2002), Multiobjective optimization using dynamic neighborhood particle swarm optimization, in, *Proceedings of the 2002 Congress on Evolutionary Computation CEC '02*, vol. 2, pp. 1677–1681, IEEE, Honolulu, Hawaii, doi:10.1109/CEC.2002.1004494.
Hu, X., R. C. Eberhart, and Y. Shi (2003), Particle swarm with extended memory for multiobjective optimization, in *IEEE Proceedings of the 2003 on Swarm Intelligence Symposium, SIS '03*, pp. 193–197, IEEE.
Huang, H., N. Cressie, and J. Gabrosek (2002), Fast, resolution-consistent spatial prediction of global processes from satellite data, *J. Comput. Graphical Stat.*, *11*(1), 63–88.
Jayakrishnan, R., R. Srinivasan, and J. G. Arnold (2004), Comparison of raingage and WSR-88D stage iii precipitation data over the Texas-Gulf basin, *J. Hydrol.*, *292*(1-4), 135–152.
Kannan, A., M. Ostendorf, W. Karl, D. Castanon, and R. Fish (2000), Ml parameter estimation of a multiscale stochastic process using the EM algorithm, *IEEE Trans. Signal Process.*, *48*(6), 1836–1840.
Kennedy, J., and R. Eberhart (1995), Particle swarm optimization, in *Proceedings of IEEE International Conference on Neural Networks*, vol. 4, pp. 1942–1948, IEEE, Perth, Western Australia.
Kumar, P. (1999), A multiple scale state-space model for characterizing subgrid scale variability of near-surface soil moisture, *IEEE Trans. Geosci. Remote Sens.*, *37*(1), 182–197.
Ly, S., C. Charles, and A. Degré (2011), Geostatistical interpolation of daily rainfall at catchment scale: The use of several variogram models in the Ourthe and Ambleve catchments, Belgium, *Hydrol. Earth Syst. Sci.*, *15*(7), 2259–2274, doi:10.5194/hess-15-2259-2011.
Montzka, C., V. R. N. Pauwels, H.-J.H. Franssen, X. Han, and H Vereecken (2012), Multivariate and multiscale data assimilation in terrestrial systems: A review, *Sensors*, *12*(12), 16,291–16,333, doi:10.3390/s121216291.
Moradkhani, H., K.-L. Hsu, H. Gupta, and S. Sorooshian (2005), Uncertainty assessment of hydrologic model states and parameters: Sequential data assimilation using the particle filter, *Water Resour. Res.*, *41*, W05012, doi:10.1029/2004WR003604.
Nan, Z. T., S. G. Wang, X. Liang, T. E. Adams, W. Teng, and Y. Liang (2010), Analysis of spatial similarities between NEXRAD and NLDAS precipitation data products, *IEEE J. Selec. Top. Appl. Earth Obs. Remote Sens.*, *3*(3), 371–385.
Parada, L., and X. Liang (2004), Optimal multiscale Kalman filter for assimilation of near-surface soil moisture into land surface models, *J. Geophys. Res.*, *109*, D24109, doi:10.1029/2004JD004745.
Parada, L. M., and X. Liang (2008), Impacts of spatial resolutions and data quality on soil moisture data assimilation, *J. Geophys. Res.*, *113*, D10101, doi:10.1029/2007JD009037.
Pitt, M. K., and N. Shephard (1999), Filtering via simulation: Auxiliary particle filters, *J. Am. Stat. Assoc.*, *94*(446), 590–599, doi:10.1080/01621459.1999.10474153.
Simone, G., F. C. Morabito, and A. Farina (2000), Radar image fusion by multiscale Kalman filtering, in *Proceedings of Third International Conference on Information Fusion FUSION 2000*, vol. 2, edited by F. C. Morabito, pp. WED3/10–WED3/17, IEEE, Paris, France.
Slatton, K., M. Crawford, and B. Evans (2001), Fusing interferometric radar and laser altimeter data to estimate surface topography and vegetation heights, *IEEE Trans. Geosci. Remote Sens.*, *39*(11), 2470–2482.
Slatton, K. C., M. Crawford, and L. Teng (2002), Multiscale fusion of INSAR data for improved topographic mapping, in *Proceedings of IEEE International Geoscience and Remote Sensing Symposium IGARSS '02*, vol. 1, edited by M. Crawford, pp. 69–71, IEEE, Toronto, Ontario, Canada.
Smith, J. A., and W. F. Krajewski (1991), Estimation of the mean field bias of radar rainfall estimates, *J. Appl. Meteorol.*, *30*(4), 397–412.
Sorooshian, S., K. L. Hsu, X. Gao, H. V. Gupta, B. Imam, and D. Braithwaite (2000), Evaluation of Persiann system satellite-based estimates of tropical rainfall, *Bull. Am. Meteorol. Soc.*, *81*(9), 2035–2046.
Tian, Y., G. J. Huffman, R. F. Adler, L. Tang, M. Sapiano, V. Maggioni, and H. Wu (2013), Modeling errors in daily precipitation measurements: Additive or multiplicative?, *Geophys. Res. Lett.*, *40*, 2060–2065, doi:10.1002/grl.50320.
Tian, Y. D., and C. D. Peters-Lidard (2010), A global map of uncertainties in satellite-based precipitation measurements, *Geophys. Res. Lett.*, *37*, L24407, doi:10.1029/2010GL046008.
Tustison, B., E. Foufoula-Georgiou, and D. Harris (2002), Scale-recursive estimation for multisensor quantitative precipitation forecast verification: A preliminary assessment, *J. Geophys. Res.*, *108*(D8), 8377, doi:10.1029/2001JD001073.
Ushio, T., et al. (2009), A Kalman filter approach to the Global Satellite Mapping of Precipitation (GSMap) from combined passive microwave and infrared radiometric data, *J. Meteorol. Soc. Jpn.*, *87*, 137–151.
Van de Vyver, H., and E. Roulin (2009), Scale-recursive estimation for merging precipitation data from radar and microwave cross-track scanners, *J. Geophys. Res.*, *114*, D08104, doi:10.1029/2008JD010709.
Voisin, N., A. W. Wood, and D. P. Lettenmaier (2008), Evaluation of precipitation products for global hydrological prediction, *J. Hydrometeorol.*, *9*(3), 388–407.
Walker, J. P, and P. R. Houser (2004), Requirements of a global near-surface soil moisture satellite mission: accuracy, repeat time, and spatial resolution, *Adv. Water Resour.*, *27*(8), 785–801.
Wang, S. (2011), Assessments of multiscale precipitation data fusion and soil moisture data assimilation and their roles in hydrological forecasts, PhD thesis, Univ. of Pittsburgh, Pittsburgh, Pa.
Wang, S., X. Liang, and Z. Nan (2011), How much improvement can precipitation data fusion achieve with a multiscale kalman smoother-based framework?, *Water Resources Research*, *47*, W00H12, doi:10.1029/2010WR009953.
Wang, X., H. Xie, H. Sharif, and J. Zeitler (2008), Validating NEXRAD MPE and Stage III precipitation products for uniform rainfall on the Upper Guadalupe River Basin of the Texas Hill Country, *J. Hydrol.*, *348*(1-2), 73–86, doi:10.1016/j.jhydrol.2007.09.057.
Willsky, A. (2002), Multiresolution Markov models for signal and image processing, *Proceedings of the IEEE*, *90*(8), 1396–1458, doi:10.1109/JPROC.2002.800717.